Macromolecules

Article

Cite This: Macromolecules 2019, 52, 1985−1992

pubs.acs.org/Macromolecules

Structure−Property Relationship of Regioregular Polytriazoles Produced by Ligand-Controlled Regiodivergent Ru(II)-Catalyzed Azide−Alkyne Click Polymerization

Die Huang,[†] Yong Liu,[‡] Anjun Qin,*[,†] and Ben Zhong Tang*[,†,‡]

[†]State Key Laboratory of Luminescent Materials and Devices, Center for Aggregation-Induced Emission, South China University of Technology, Guangzhou 510640, China

[‡]Department of Chemistry, Hong Kong Branch of Chinese National Engineering Research Centre for Tissue Restoration and Reconstruction, Institute for Advanced Study, and Department of Chemical and Biological Engineering, The Hong Kong University of Science & Technology (HKUST), Clear Water Bay, Kowloon, Hong Kong, China

Supporting Information

ABSTRACT: Exploitation of new polymerization with selectivity is of significance to the preparation of functional polymers and the study of their structure−property relationship. In this work, we successfully developed an efficient Ru(II)-catalyzed azide−alkyne click polymerization (RuAACP), of which the regioselectivity can be switched by the ligands on the Ru(II) catalysts. With $RuH_2(CO)(PPh_3)_3$ as catalyst, 1,4-regioregular polytriazoles (PTAs) with high weight-average molecular weights (M_w up to 15300) and high 1,4-regioregularities (the fraction of 1,4-isomer, $F_{1,4}$ up to 100%) were produced in satisfactory yields (up to 97.6%). In contrast, $Cp^*Ru(PPh_3)_2Cl$-catalyzed AACP facilely yielded (up to 98.3%) 1,5-regioregular PTAs with high M_w (up to 15520) and $F_{1,5}$ (up to 100%). All the obtained PTAs exhibit good solubility and high thermal stability. The glass transition temperature (T_g) of 1,4-regioregular PTA is much higher than that of its 1,5-regioregular counterpart, revealing the considerable effect of the regiostructure on their T_g. Both 1,4- and 1,5-regioregular PTAs containing tetraphenylethene moieties in their backbones show aggregation-induced emission features. In addition, the impact of regiostructure on the light refractivity of the PTAs was also investigated, and 1,4-regioregular PTA possesses higher refractivity indices than 1,5-regioregular PTA.

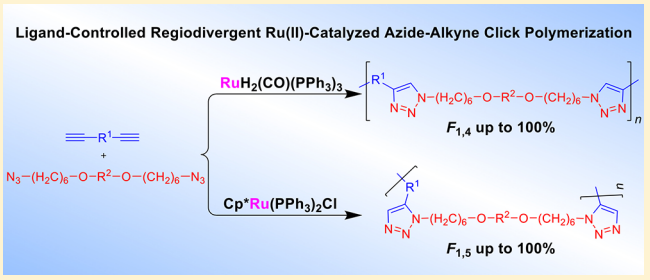

INTRODUCTION

The development of new effective and selective polymerizations for the synthesis of polymers with well-defined structures and unique properties is an important topic in the field of polymer science.[1,2] Generally, new polymerization could be developed on the basis of organic reaction with remarkable features of high efficiency, moderate reaction conditions, readily available reactants, and effective catalysts.[3] Since it was introduced by Sharpless and co-workers in 2001, click chemistry has inspired a lot of scientists in diverse areas.[4−18] Click reactions are a group of nearly prefect reactions which enjoy numerous excellent features, such as high efficiency, atom economy, selectivity, great functionality tolerance, simple reaction conditions, and simple product isolation.[4] Thanks to their great click characteristics, click reactions have drawn increasing attention of polymer chemists, and some of them have been successfully developed into powerful polymerization techniques, i.e., click polymerizations,[19] including azide−alkyne click polymerization (AACP),[20−24] thiol−ene/yne click polymerization,[25−29] Diels−Alder click polymerization,[30−32] and the emerging amino−yne and hydroxyl−yne click polymerizations.[33,34]

In particular, the famous Cu(I)-catalyzed azide−alkyne click polymerization (CuAACP), evolved from the archetypal click reaction of Cu(I)-catalyzed azide−alkyne cycloaddition (CuAAC), has been systematically investigated and found extensive applications in various areas, such as self-healing materials, self-assembly materials, shape memory materials, nonlinear optical materials, photoelectric materials, and biomaterials.[35−46] In contrast, AACP catalyzed by other metal catalysts is rarely reported. To the best of our knowledge, besides CuAACP, only Ru(II)-catalyzed azide−alkyne click polymerization (RuAACP) with $Cp^*Ru(PPh_3)_2Cl$ or $[Cp^*RuCl_2]_n$ as catalyst was reported as metal-catalyzed AACP by our group in 2008.[47] The $Cp^*Ru(PPh_3)_2Cl$-/$[Cp^*RuCl_2]_n$-catalyzed AACP proceed in a 1,5-regioselective manner, which is different from the 1,4-regioselective manner of CuAACP. Meanwhile, RuAACP is more suitable than CuAACP in some special cases. For example, polytriazoles (PTAs) containing Mo−Mo metal bonds in the polymer

Received: December 15, 2018
Revised: February 9, 2019
Published: February 22, 2019

DOI: 10.1021/acs.macromol.8b02671
Macromolecules 2019, 52, 1985−1992

Scheme 1. Ru(II)-Catalyzed Azide−Alkyne Click Polymerization for the Preparation of 1,4- and 1,5-Regioregular Polytriazoles

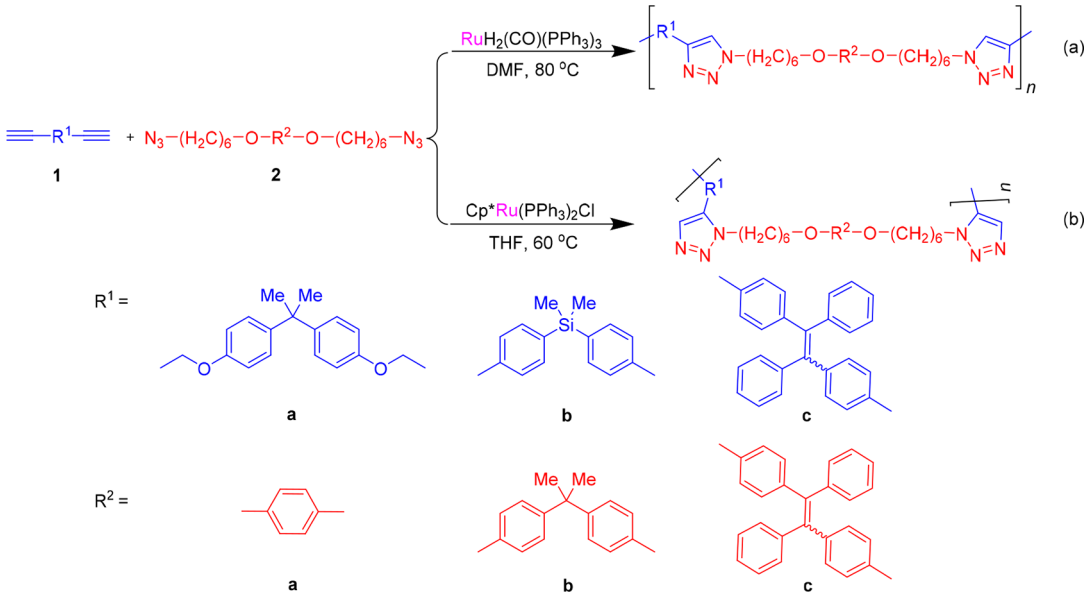

chains could be successfully prepared via RuAACP; however, because of the disproportionation of the Mo−Mo metal bonds, these PTAs could not be obtained by CuAACP.[48] Therefore, the establishment of new efficient metal-catalyzed AACPs can bring new synthetic methods for PTAs as well as new opportunities for AACPs.

In addition to the aforementioned Cu(I) and Ru(II) catalysts, numerous catalysts based on various metals, including Ag, Au, Ir, Ni, Zn, and Ln, have also been applied to catalyze azide−alkyne cycloaddition.[49] What is more exciting, Jia et al. reported that the regioselectivity of Ru(II)-catalyzed azide−alkyne cycloaddition could be controlled by the ligands.[50,51] Specifically, $RuH_2(CO)(PPh_3)_3$ can catalyze the azide−alkyne cycloaddition to selectively generate 1,4-disubstituted triazoles.[52,53] Inspired by Jia's work, we surmised that this click reaction could be developed into a brand new RuAACP for the preparation of 1,4-regioregular PTAs, which will greatly expand the scope of RuAACP and serve as a powerful tool for the structure−property relationship study of PTAs.

In this work, we successfully established a novel and effective RuAACP (Scheme 1a) which shows inverse regioselectivity compared with previously reported one (Scheme 1b). 1,4-Regioregular PTAs with high molecular weights (M_w up to 15300) and high regioregularities (the fraction of 1,4-isomer, $F_{1,4}$ up to 100%) were obtained in satisfactory yields (up to 97.6%) via RuAACP using $RuH_2(CO)(PPh_3)_3$ as catalyst. Meanwhile, 1,5-regioregular PTA was also prepared by the previous reported $Cp^*Ru(PPh_3)_2Cl$-catalyzed AACP. All of the produced PTAs enjoy good solubility and excellent thermal stability. Thanks to the high efficiency and great functional tolerance, this RuAACP could be used to prepare PTAs with aggregation-induced emission (AIE) features by introducing AIE-active tetraphenylethene (TPE) moieties into the polymer chains.[54,55] The structure−property relationship study indicated that 1,4- and 1,5-regioregular PTAs showed some differences in thermal property, photophysical property, and light refractivity.

RESULTS AND DISCUSSION

Click Polymerization. To develop the unconventional RuAACP for the preparation of 1,4-regioregular PTAs, diynes **1** and diazides **2** were designed and synthesized following the literature methods. Spectroscopic methods were applied to characterize the structures of all the monomers, and satisfactory analysis results were obtained (see the Supporting Information for details). The typical polymerization propagated smoothly in *N*,*N*-dimethylformamide (DMF) at 80 °C in the presence of $RuH_2(CO)(PPh_3)_3$ under nitrogen.

To obtain soluble PTAs with high molecular weights and high regioregularities, the polymerization conditions were systematically optimized using **1a** and **2a** as model monomers. The time course of the polymerization was first investigated in tetrahydrofuran (THF) (Table S1). Both M_w and yields of the produced PTAs increased with prolonging the reaction time. In consideration of the polymerization results and time cost, 18 h was adopted as the reaction time for further research.

We then studied the effect of monomer concentration on the polymerization (Table S2). Enhancing the monomer concentration from 0.1 to 0.5 M had a positive impact on the polymerization results, which was reasonable since intermolecular monomer collisions could be facilitated by higher monomer concentration. When the monomer concentration was 0.5 M, PTA with moderate molecular weight of 7390 was obtained in high yield (94.8%). Further increasing monomer concentration to 1.0 M resulted in gelation, and only insoluble gel was yielded. Hence, we chose 0.5 M as the optimal monomer concentration.

As an important polymerization parameter, the loading effect of the catalyst on the polymerization was also evaluated (Table S3). The results showed that the catalyst loading exerted a strong influence on the solubility of the products. With the increment of the catalyst loading, higher M_w and higher yields were obtained. However, when the catalyst loading was higher than or equal to 3 mol % against **1a**, the solubility of the obtained PTAs was poor probably due to the coordination between the catalyst and the formed triazoles. Therefore, based on the polymerization efficiency and economical consideration, 2 mol % against **1a** was preferred as the catalyst loading.

DOI: 10.1021/acs.macromol.8b02671
Macromolecules 2019, 52, 1985−1992

Moreover, the solvent impact on the polymerization was examined (Table S4). The polymerizations propagated smoothly in THF and dimethyl sulfoxide (DMSO), furnishing soluble PTAs with similar M_w and regioregularities in similar yields. In contrast, the polymerization in DMF offered partly soluble PTA of which the soluble part showed a highest M_w of 12250 and a $F_{1,4}$ of 95.2% compared with the PTAs from the polymerizations in THF and DMSO. We considered that the poor solubility could be ascribed to the high molecular weight and anticipated that soluble PTAs could be obtained by shortening the reaction time in DMF. To verify our expectation, we performed a series of experiments tracking the time course of the polymerization in DMF (Table S5). Delightedly, soluble PTA with M_w as high as 10650 and $F_{1,4}$ as high as 97.1% was successfully obtained in a high yield (93.3%) after only 5 h (Table S5, entry 3). Therefore, DMF and 5 h were chosen as the optimal solvent and reaction time, respectively.

With these optimum polymerization conditions in hand, we used different diynes and diazides as monomers to test the robustness of this new RuAACP and to enrich the polymer structures (Table 1, entries 1 and 4–8). All the polymerizations performed well in DMF at 80 °C, furnishing soluble 1,4-regioregular PTAs ($F_{1,4}$ = 95.6–100%) with high M_w (up to 15300) in high yields (up to 97.6%). Interestingly, when aromatic alkynes were used as diyne monomers, the $F_{1,4}$ of the resulting PTAs was 100%, indicating the regiospecificity of this polymerization of aromatic alkyne possibly because of the steric hindrance. These results demonstrated that a novel and facile RuAACP was successfully developed for the preparation of 1,4-regioregular PTAs.

Table 1. Polymerizations of Diynes 1 and Diazides 2[a]

entry	monomers	polymer	yield (%)	M_w[b]	$Đ$[b]	$F_{1,4}$[c] (%)
1	**1a** + **2a**	P**1a2a**	93.3	10650	1.70	97.1
2[d]	**1a** + **2a**	P**1a2a**′	41.0	3580	1.27	2[e]
3[f]	**1a** + **2a**	P**1a2a**″	98.2	13510	1.48	100
4	**1a** + **2b**	P**1a2b**	79.4	7710	1.52	96.2
5	**1a** + **2c**	P**1a2c**	97.6	10900	1.66	95.6
6	**1b** + **2a**	P**1b2a**	89.2	10250	1.79	100
7	**1c** + **2a**	P**1c2a**	83.5	9430	1.64	100
8[g]	**1c** + **2a**	P**1c2a**	91.5	15300	2.02	100
9[h]	**1c** + **2a**	P**1c2a**′	98.3	15520	2.01	0[i]

[a]Carried out under nitrogen in DMF at 80 °C for 5 h, [**1**]/[**2**] = 1, [**1**] = 0.5 M, $[RuH_2(CO)(PPh_3)_3]$ = 0.02[**1**]. [b]Estimated by advanced polymer chromatography (APC) in THF on the basis of polystyrene calibration, polydispersity indices $Đ = M_w/M_n$. [c]Estimated from ^{1}H NMR spectra. [d]Carried out under nitrogen in THF at 60 °C for 12 h, [**1a**]/[**2a**] = 1, [**1a**] = 0.2 M, $[Cp^*Ru(PPh_3)_2Cl]$ = 0.04[**1a**]. [e]$F_{1,5}$ = 98%. [f]Carried out under nitrogen in THF at 60 °C for 12 h, [**1a**]/[**2a**] = 1, [**1a**] = 0.1 M, $[Cu(PPh_3)_3Br]$ = 0.1[**1a**]. [g]Carried out in DMF at 80 °C for 12 h. [h]Carried out under nitrogen in THF at 60 °C for 5 h, [**1c**]/[**2a**] = 1, [**1c**] = 0.2 M, $[Cp^*Ru(PPh_3)_2Cl]$ = 0.04[**1c**]. [i]$F_{1,5}$ = 100%.

Structural Characterization. The obtained PTAs possessed good solubility in commonly used organic solvents, such as THF, DMSO, and DMF, which facilitates to characterize their structures by standard "wet" spectroscopic methods. Herein, the Fourier transformed infrared (FT-IR) and proton and carbon nuclear magnetic resonance (NMR) spectra were used. Considering the similar spectral profiles of the resultant polymers (Figures 1–3 and Figures S1–S12), the structural illustration of P**1a2a** is shown below as an example.

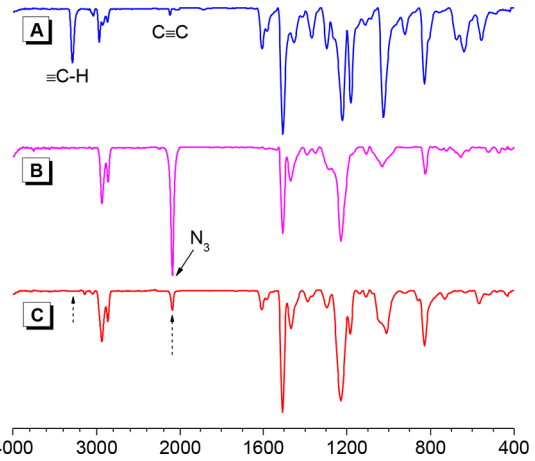

Figure 1. FT-IR spectra of (A) monomer **1a**, (B) monomer **2a**, and (C) polymer P**1a2a**.

The FT-IR spectrum of P**1a2a** is displayed in Figure 1, and for comparison, the spectra of its corresponding monomers **1a** and **2a** are given in the same figure. The absorption band observed at 3286 cm^{-1} in the FT-IR spectrum of **1a** was assignable to the vibrational stretching of ≡C–H, which was absent in the spectrum of P**1a2a**. Meanwhile, compared to that of **2a**, the spectrum of P**1a2a** exhibited a very weak absorption band at 2095 cm^{-1} associated with the stretching vibration of the N_3 group. These results indicate the almost complete consumption of the ethynyl and azido groups of the monomers, suggestive of the occurrence of the polymerization.

More detailed information about the polymer structure could be found through the ^{1}H and ^{13}C NMR analysis. To gain insight into the structures of the resultant PTAs and figure out the regioregularities, 1,5-regioregular PTA P**1a2a**′ and 1,4-regioregular PTA P**1a2a**″ were prepared by conventional $Cp^*Ru(PPh_3)_2Cl$- and $Cu(PPh_3)_3Br$-catalyzed AACPs, respectively (see the Supporting Information for details). Figure 2 shows the ^{1}H NMR spectra of P**1a2a**, P**1a2a**′, and P**1a2a**″ and their monomers (**1a** and **2a**) in deuterated DMSO (DMSO-d_6). The acetylene protons of monomer **1a** resonated at δ 3.55 almost completely disappeared in the spectrum of P**1a2a**, indicating the consumption of monomer **1a** and substantiating the conclusion drawn from the above FT-IR analysis. The peaks at δ 4.74 and 3.32 assigned to the methylene protons of **1a** and the protons of methylene adjacent to azide group of **2a** shifted to δ 5.06 and 4.34 in the spectrum of P**1a2a**, respectively. Similar variations could be observed in the spectrum of P**1a2a**″. Moreover, a new sharp peak (a) emerged at δ 8.19 in the spectrum of P**1a2a**, which could be associated with the resonance of the proton of 1,4-disubstituted 1,2,3-triazole ring by referring to the spectrum of P**1a2a**″. By comparing the spectra of P**1a2a** and P**1a2a**′, an extremely small peak (b) related to the resonance of the proton of 1,5-disubstituted 1,2,3-triazole ring was noticed in the spectrum of P**1a2a** at δ 7.80. Based on the above analysis, the calculation of the polymer regioregularity could be achieved by using the integrals of peaks (a) and (b). The $F_{1,4}$ of P**1a2a** was calculated to be 97.1%, indicative of the excellent 1,4-regioselectivity of this new RuAACP.

DOI: 10.1021/acs.macromol.8b02671
Macromolecules 2019, 52, 1985–1992

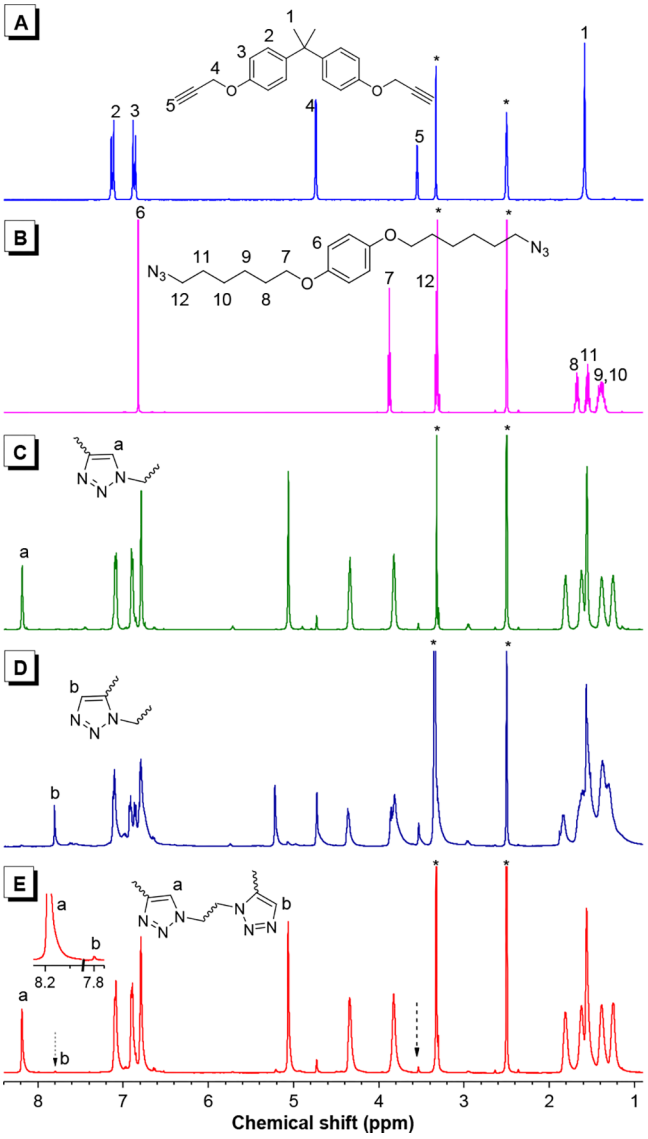

Figure 2. ^{1}H NMR spectra of (A) monomer **1a**, (B) monomer **2a**, (C) polymer P**1a2a**″, (D) polymer P**1a2a**′, and (E) polymer P**1a2a** in DMSO-d_6. The solvent peaks are marked with asterisks.

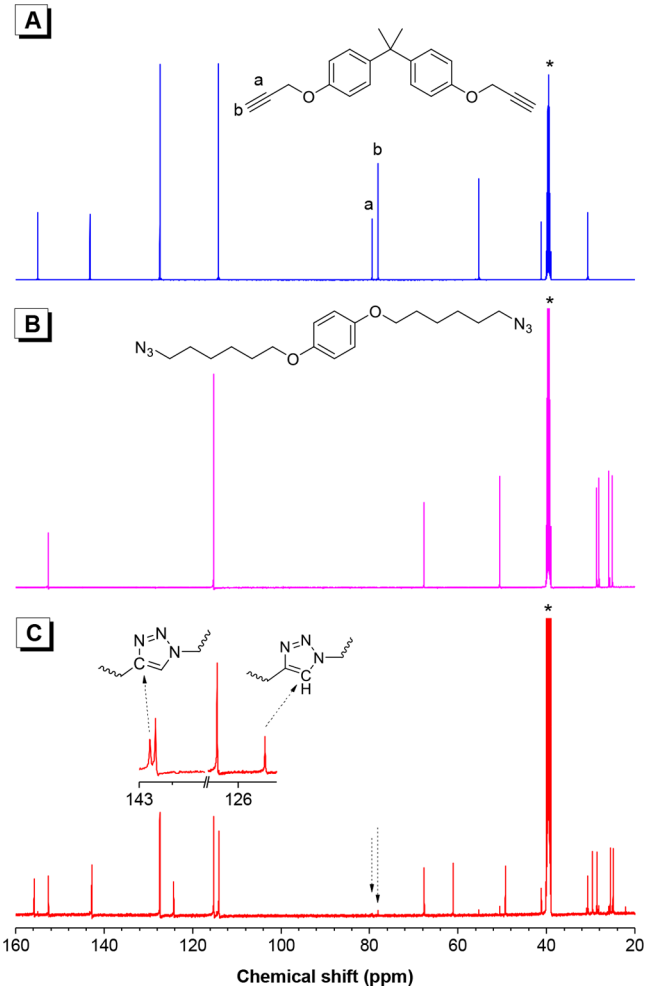

Figure 3. ^{13}C NMR spectra of (A) monomer **1a**, (B) monomer **2a**, and (C) polymer P**1a2a** in DMSO-d_6. The solvent peaks are marked with asterisks.

The ^{13}C NMR spectra of P**1a2a** and its monomers **1a** and **2a** are depicted in Figure 3 for further verification of the polymeric structure. The resonance peaks of ethynyl carbons of **1a** at δ 79.44 and 78.07 almost could not be observed in the spectrum of P**1a2a**. In addition, two new resonance peaks that arose from the carbons of the formed triazole ring appeared at δ 142.84 and 124.26 in the spectrum of P**1a2a**. The successful occurrence of this RuAACP was confirmed by these results once again.

Thermal Properties. The thermal stability of the PTAs was studied by thermogravimetric analysis (TGA). As shown in Figure 4A, the decomposition temperatures (T_d) of the resultant PTAs for 5% weight loss under nitrogen are higher than 352 °C, suggestive of the high thermal stability of these PTAs. Noteworthy, 1,4-regioregular P**1c2a** and the corresponding 1,5-regioregular P**1c2a**′ showed very similar TGA thermograms and possessed similar T_d of 375.1 and 368.3 °C, respectively. For further studying the relationship between the regiostructure and thermal property, the glass transition temperatures (T_g) of P**1c2a** and P**1c2a**′ were evaluated using differential scanning calorimetry (DSC) measurement. As shown in Figure 4B, the T_g of P**1c2a** is nearly 40 °C higher than that of P**1c2a**′, which could be ascribed to the less steric hindrance of 1,4-isomer and its more planar structure facilitating the close packing of the polymer chains. These results exposed that the regioregularity of PTA has a negligible influence on the T_d but a noticeable impact on the T_g and 1,5-regiostructure can greatly reduce the T_g of PTA because of its more twisted conformation.

Photophysical Properties. Taking P**1c2a** and P**1c2a**′ as examples, the structure−photophysical property relationship of PTAs was methodically investigated by measuring their absorption and emission spectra in dilute solutions. As displayed in Figure 5A, P**1c2a** and P**1c2a**′ showed similar absorption spectra, and their absorption maxima were observed at 333 and 325 nm, respectively. Meanwhile, as shown in Figure 5B, the photoluminescence (PL) spectrum of P**1c2a** peaked at 501 nm was 10 nm red-shifted from that of P**1c2a**′, suggestive of an enhanced electronic communication between tetraphenylethylene (TPE) and triazole units in 1,4-regioregular PTA. These changes in the absorption and PL spectra of 1,4- and 1,5-regioregular PTAs are in agreement with the previous report,[47] which can be explained by the more conjugated structure of 1,4-regioregular PTA because of the

DOI: 10.1021/acs.macromol.8b02671
Macromolecules 2019, 52, 1985−1992

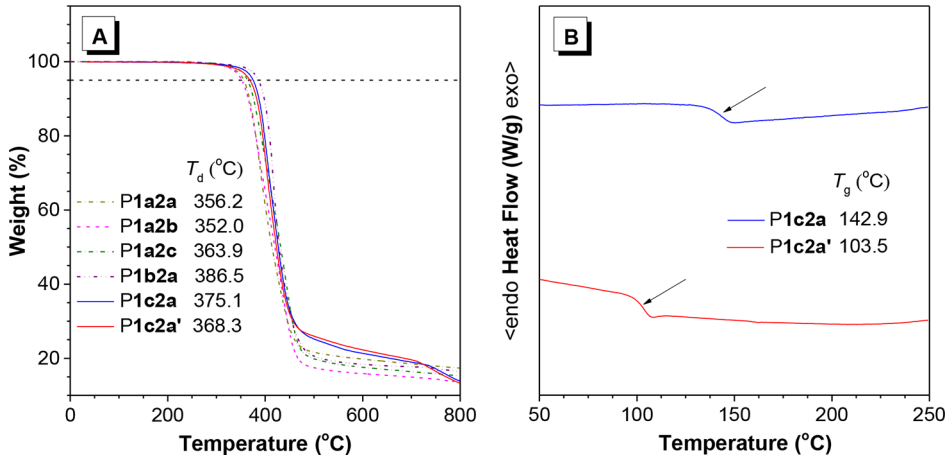

Figure 4. (A) TGA thermograms of the resultant PTAs. (B) DSC thermograms of P**1c2a** and P**1c2a**′ with similar M_w.

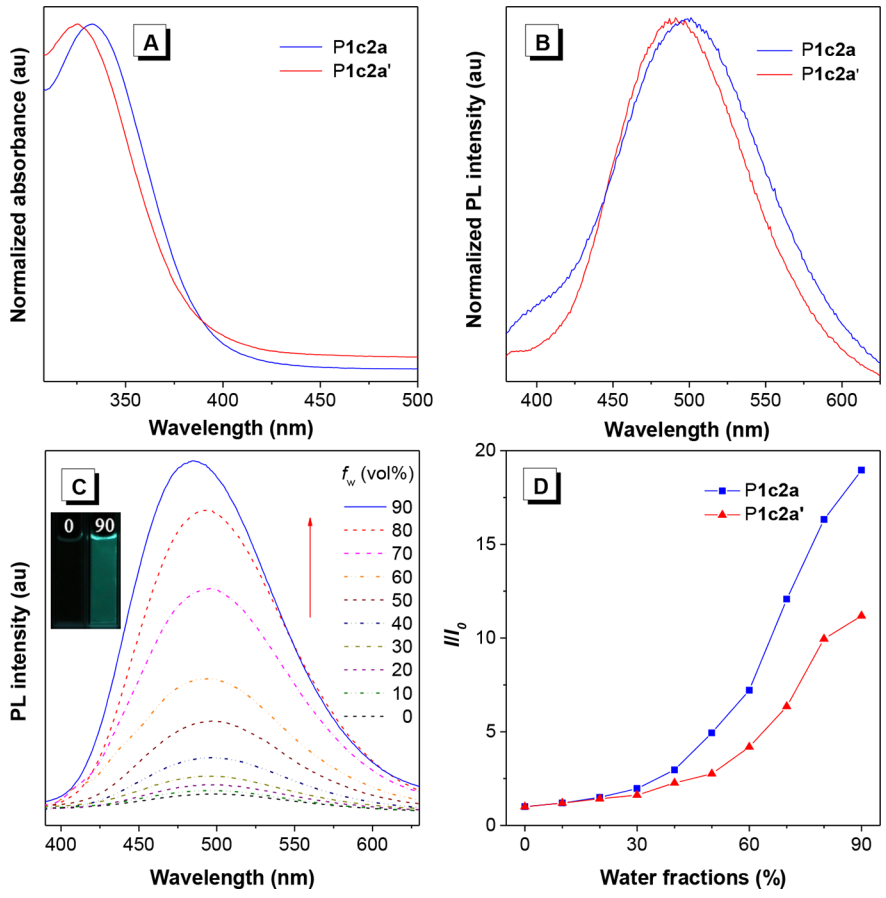

Figure 5. Normalized (A) absorption and (B) PL spectra of P**1c2a** and P**1c2a**′ in THF solution. (C) PL spectra of P**1c2a** in THF and THF/water mixtures with different water fractions (f_w). Inset: photograph taken under illumination of hand-held UV lamp. (D) Plots of I/I_0 of P**1c2a** and P**1c2a**′ versus water fraction, where I = peak intensity and I_0 = peak intensity at f_w = 0. Concentrations: 10 μM; excitation wavelength: 333 nm for P**1c2a** and 325 nm for P**1c2a**′.

less steric hindrance and the more planar conformation of 1,4-isomer compared with its 1,5-regioregular counterpart.

Being a hot research topic in recent years, aggregation-induced emission (AIE) is coined for a unique photophysical phenomenon that some propeller-shaped luminogens show very weak or no emission in their dilute solutions but intensely fluoresce in the aggregate state, which is opposite to the conventional aggregation-caused quenching (ACQ) effect.[56−59] At present, the most accepted mechanism for AIE system is the restriction of intramolecular motion (RIM) in the aggregate state, including the restriction of intramolecular rotation (RIR) and intramolecular vibration (RIV), which reduces the nonradiative decay rate of the excited state to turn on the luminescence. As one of the most famous AIE-active luminogens, TPE was usually introduced into polymer chains to endow the polymers with AIE features.[60,61] CuAACP and metal-free click polymerizations of activated monomers have been developed into powerful tools for the preparation of AIE-

DOI: 10.1021/acs.macromol.8b02671
Macromolecules 2019, 52, 1985−1992

active polymers with TPE units.[62−66] However, using RuAACP to prepare AIE-active polymers has not been reported yet. Meanwhile, although the influence of linking manner of 1,4-disubstituted triazole ring on the emission properties of PTAs has been investigated in previous report,[67] the regiostructure effect on the AIE characteristics of PTAs still remains to be studied.

Thanks to the great functional tolerance of both $RuH_2(CO)(PPh_3)_3$- and $Cp^*Ru(PPh_3)_2Cl$-catalyzed AACPs, TPE moieties were successfully incorporated into the polymer chains of P**1c2a** and P**1c2a′**. As a rule of thumb, we anticipated that both P**1c2a** and P**1c2a′** would inherit the AIE features of TPE. To confirm this anticipation, we first compared the fluorescence of P**1c2a** in the solution and aggregate states under the 365 nm UV irradiation. As shown in the inset of Figure 5C, almost no fluorescence was observed when P**1c2a** was molecularly dissolved in THF. Conversely, a relatively strong fluorescence could be observed when large amount of poor solvent of water was added into the THF solution. Encouraged by this preliminary result, we then investigated the emission behavior of P**1c2a** systematically. As exhibited in Figure 5C, the PL spectrum of P**1c2a** in THF solution was nearly parallel with the abscissa axis, illustrating the very weak emission in good solvent. With increasing the water fractions (f_w) of THF/water mixtures, the PL intensity enhanced gradually and reached the highest level at a f_w of 90% (I_{90}), which was 18-fold higher than that in THF (I_0) (Figure 5D). Such emission behavior is a typical AIE process, demonstrating that P**1c2a** is AIE-active. At the same time, the similar PL behavior of P**1c2a′** in THF/water mixtures with different f_w (Figure 5D and Figure S13) also indicated its AIE features. The aforementioned RIM mechanism can be applied to explain the AIE characteristics of P**1c2a** and P**1c2a′**. Notably, the I_{90} of P**1c2a′** was only 10-fold higher than its I_0, suggestive of the weaker AIE effect (the extent of emission enhancement) of P**1c2a′** compared to that of P**1c2a**, which probably could be attributed to the enhanced steric effect of the 1,5-isomer.[68,69] These results indicated that the regiostructures of PTAs have almost no influence on their AIE nature but observable impact on their AIE effect.

Apart from P**1c2a** and P**1c2a′**, we also studied the PL behavior of P**1a2c** bearing TPE units in its backbone in THF/water mixtures with different f_w. As shown in Figure S14, the PL intensity of P**1a2c** increased with the addition of water into its THF solution, revealing that P**1a2c** is also AIE-active.

Light Refractivity. High refractive index (n) polymers with the advantages of light weight, processability, and impact resistance have drawn an increasing attention because of their widespread applications in the fields of optics and photoelectricity, such as lenses, waveguides, antireflective coatings, photoresists, and encapsulants for organic light-emitting diodes.[70] Because the introduction of aromatic rings and polarizable π-conjugated functionalities into the polymers is theoretically beneficial to the improvement of their refractive indices,[71] we anticipated that P**1c2a** and P**1c2a′** containing plentiful aromatic rings and polarized triazole rings would exhibit high refractive indices. Thanks to their good solubility and film-forming ability, thin films of P**1c2a** and P**1c2a′** were manufactured successfully on silica wafers by the spin-coating process, and the results of wavelength-dependent refractivity measurements are displayed in Figure 6. In a wide spectral region of 400−1700 nm, both the thin films of P**1c2a** and P**1c2a′** with thickness of 386.3 and 396.1 nm show high n values of 1.748−1.615 and 1.720−1.607, respectively. Meanwhile, their n values at 632.8 nm ($n_{632.8}$) are 1.644 and 1.634, which are much higher than those of conventional optical plastics, such as polystyrene ($n_{632.8}$ = 1.588), polycarbonate ($n_{632.8}$ = 1.580), and poly(methyl methacrylate) ($n_{632.8}$ = 1.489).[72] Compared with 1,5-regioregular P**1c2a′**, 1,4-regioregular P**1c2a** shows higher n values because of its higher conjugated structure and higher stacking density,[70] indicating that the n values of PTAs can be fine-tuned by their regiostructures.

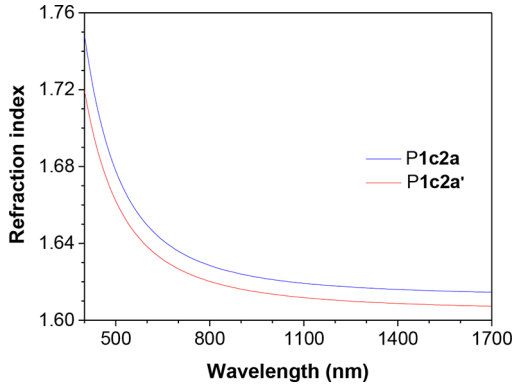

Figure 6. Wavelength-dependent refractive indices of the thin films of polymers P**1c2a** and P**1c2a′**.

CONCLUSIONS

In summary, we have successfully established a 1,4-regioselective RuAACP by altering the ligands on Ru(II) complex and using $RuH_2(CO)(PPh_3)_3$ as catalyst. Soluble and thermally stable 1,4- and 1,5-regioregular PTAs with high molecular weights and regioregularities were obtained in high yields by the $RuH_2(CO)(PPh_3)_3$-/$Cp^*Ru(PPh_3)_2Cl$-catalyzed AACPs, respectively, suggestive of the ligand-dependent regioselectivity in the RuAACP. The relationships between the regiostructures of PTAs and their thermal, photophysical, and optical properties were systematically studied. It was found that the regiostructures of PTAs have a noticeable influence on their T_g, and 1,4-regioregular PTA showed a higher T_g than its 1,5-regioregular analogue. By introduction of TPE units into the polymer chains, AIE-active 1,4- and 1,5-regioregular PTAs were obtained. Owing to its more conjugated structure, 1,4-regioregular PTA exhibits a higher refractive index than that of the 1,5-regioregular one. This work not only provides a new method for the preparation of 1,4-regioregular PTAs but also offers a new platform for investigation of structure−property relationship of PTAs.

ASSOCIATED CONTENT

Supporting Information

The Supporting Information is available free of charge on the ACS Publications website at DOI: 10.1021/acs.macromol.8b02671.

Experimental details, optimization of reaction conditions, and characterization data (FT-IR, NMR, PL) (PDF)

AUTHOR INFORMATION

Corresponding Authors

*E-mail: msqinaj@scut.edu.cn (A.J.Q.).

DOI: 10.1021/acs.macromol.8b02671
Macromolecules 2019, 52, 1985−1992

*E-mail: tangbenz@ust.hk (B.Z.T.).

ORCID

Anjun Qin: 0000-0001-7158-1808

Ben Zhong Tang: 0000-0002-0293-964X

Notes

The authors declare no competing financial interest.

■ ACKNOWLEDGMENTS

This work was financially supported by the National Natural Science Foundation of China (21788102, 21525417, and 21490571), the National Program for Support of Top-Notch Young Professionals, the Natural Science Foundation of Guangdong Province (2016A030312002), the Fundamental Research Funds for the Central Universities (2015ZY013), and the Innovation and Technology Commission of Hong Kong (ITC-CNERC14S01).

■ REFERENCES

(1) Matyjaszewski, K.; Xia, J. Atom Transfer Radical Polymerization. *Chem. Rev.* **2001**, *101*, 2921−2990.

(2) Tang, B. Z. Construction of Functional Polymers from Acetylenic Triple-Bond Building Blocks. *Macromol. Chem. Phys.* **2008**, *209*, 1303−1307.

(3) Qin, A.; Liu, Y.; Tang, B. Z. Regioselective Metal-Free Click Polymerization of Azides and Alkynes. *Macromol. Chem. Phys.* **2015**, *216*, 818−828.

(4) Kolb, H. C.; Finn, M. G.; Sharpless, K. B. Click Chemistry: Diverse Chemical Function from a Few Good Reactions. *Angew. Chem., Int. Ed.* **2001**, *40*, 2004−2021.

(5) Finn, M. G.; Fokin, V. V. Click Chemistry: Function Follows Form. *Chem. Soc. Rev.* **2010**, *39*, 1231−1232.

(6) Golas, P. L.; Matyjaszewski, K. Marrying Click Chemistry with Polymerization: Expanding the Scope of Polymeric Materials. *Chem. Soc. Rev.* **2010**, *39*, 1338−1354.

(7) Thirumurugan, P.; Matosiuk, D.; Jozwiak, K. Click Chemistry for Drug Development and Diverse Chemical-Biology Applications. *Chem. Rev.* **2013**, *113*, 4905−4979.

(8) Haque, M. M.; Peng, X. DNA-Associated Click Chemistry. *Sci. China: Chem.* **2014**, *57*, 215−231.

(9) Tang, W.; Becker, M. L. Click" Reactions: A Versatile Toolbox for the Synthesis of Peptide-Conjugates. *Chem. Soc. Rev.* **2014**, *43*, 7013−7039.

(10) Xi, W.; Scott, T. F.; Kloxin, C. J.; Bowman, C. N. Click Chemistry in Materials Science. *Adv. Funct. Mater.* **2014**, *24*, 2572−2590.

(11) Marrocchi, A.; Facchetti, A.; Lanari, D.; Santoro, S.; Vaccaro, L. Click-Chemistry Approaches to π-Conjugated Polymers for Organic Electronics Applications. *Chem. Sci.* **2016**, *7*, 6298−6308.

(12) Meyer, J. P.; Adumeau, P.; Lewis, J. S.; Zeglis, B. M. Click Chemistry and Radiochemistry: The First 10 Years. *Bioconjugate Chem.* **2016**, *27*, 2791−2807.

(13) Tiwari, V. K.; Mishra, B. B.; Mishra, K. B.; Mishra, N.; Singh, A. S.; Chen, X. Cu-Catalyzed Click Reaction in Carbohydrate Chemistry. *Chem. Rev.* **2016**, *116*, 3086−3240.

(14) Martens, S.; Holloway, J. O.; Du Prez, F. E. Click and Click-Inspired Chemistry for the Design of Sequence-Controlled Polymers. *Macromol. Rapid Commun.* **2017**, *38*, 1700469.

(15) Cañeque, T.; Müller, S.; Rodriguez, R. Visualizing Biologically Active Small Molecules in Cells Using Click Chemistry. *Nat. Rev. Chem.* **2018**, *2*, 202−215.

(16) Xu, Z.; Bratlie, K. M. Click Chemistry and Material Selection for in Situ Fabrication of Hydrogels in Tissue Engineering Applications. *ACS Biomater. Sci. Eng.* **2018**, *4*, 2276−2291.

(17) Zheng, Y.; Li, S.; Weng, Z.; Gao, C. Hyperbranched Polymers: Advances from Synthesis to Applications. *Chem. Soc. Rev.* **2015**, *44*, 4091−4130.

(18) Huang, Z.; Zhou, Y.; Wang, Z.; Li, Y.; Zhang, W.; Zhou, N.; Zhang, Z.; Zhu, X. Recent Advances of CuAAC Click Reaction in Building Cyclic Polymer. *Chin. J. Polym. Sci.* **2017**, *35*, 317−341.

(19) Qin, A.; Lam, J. W. Y.; Tang, B. Z. Click Polymerization. *Chem. Soc. Rev.* **2010**, *39*, 2522−2544.

(20) Qin, A.; Lam, J. W. Y.; Tang, B. Z. Click Polymerization: Progresses, Challenges, and Opportunities. *Macromolecules* **2010**, *43*, 8693−8702.

(21) Li, H.; Sun, J.; Qin, A.; Tang, B. Z. Azide-Alkyne Click Polymerization: An Update. *Chin. J. Polym. Sci.* **2012**, *30*, 1−15.

(22) Shi, Y.; Cao, X.; Gao, H. The Use of Azide-Alkyne Click Chemistry in Recent Syntheses and Applications of Polytriazole-Based Nanostructured Polymers. *Nanoscale* **2016**, *8*, 4864−4881.

(23) Shi, Y.; Sun, J.; Qin, A. Click Polymerization: The Aurora of Polymer Synthetic Methodology. *J. Polym. Sci., Part A: Polym. Chem.* **2017**, *55*, 616−621.

(24) Huang, D.; Qin, A.; Tang, B. Z. Hyperbranched Polymers Prepared by Alkyne-Based Click Polymerization. *Acta Polym. Sin.* **2017**, *2*, 178−199.

(25) Lowe, A. B. Thiol-Ene "Click" Reactions and Recent Applications in Polymer and Materials Synthesis. *Polym. Chem.* **2010**, *1*, 17−36.

(26) Lowe, A. B. Thiol-Ene "Click" Reactions and Recent Applications in Polymer and Materials Synthesis: A First Update. *Polym. Chem.* **2014**, *5*, 4820−4870.

(27) Machado, T. O.; Sayer, C.; Araujo, P. H. H. Thiol-Ene Polymerisation: A Promising Technique to Obtain Novel Biomaterials. *Eur. Polym. J.* **2017**, *86*, 200−215.

(28) Lowe, A. B.; Hoyle, C. E.; Bowman, C. N. Thiol-Yne Click Chemistry: A Powerful and Versatile Methodology for Materials Synthesis. *J. Mater. Chem.* **2010**, *20*, 4745−4750.

(29) Yao, B.; Sun, J.; Qin, A.; Tang, B. Z. Thiol-Yne Click Polymerization. *Chin. Sci. Bull.* **2013**, *58*, 2711−2718.

(30) Tasdelen, M. A. Diels-Alder "Click" Reactions: Recent Applications in Polymer and Material Science. *Polym. Chem.* **2011**, *2*, 2133−2145.

(31) Gandini, A. The Furan/Maleimide Diels-Alder Reaction: A Versatile Click-Unclick Tool in Macromolecular Synthesis. *Prog. Polym. Sci.* **2013**, *38*, 1−29.

(32) Gaso-Sokac, D.; Stivojevic, M. Diels-Alder "Click" Reactions. *Curr. Org. Chem.* **2016**, *20*, 2211−2221.

(33) Huang, D.; Liu, Y.; Qin, A.; Tang, B. Z. Recent Advances in Alkyne-Based Click Polymerizations. *Polym. Chem.* **2018**, *9*, 2853−2867.

(34) Li, B.; Huang, D.; Qin, A.; Tang, B. Z. Progress on Catalytic Systems Used in Click Polymerization. *Macromol. Rapid Commun.* **2018**, *39*, 1800098.

(35) Huang, D.; Qin, A.; Tang, B. Z. In *Click Polymerization*; The Royal Society of Chemistry: 2018; Chapter 2, pp 36−85.

(36) Doehler, D.; Michael, P.; Binder, W. H. Cuaac-Based Click Chemistry in Self-Healing Polymers. *Acc. Chem. Res.* **2017**, *50*, 2610−2620.

(37) McIntosh, J. T.; Nazemi, A.; Bonduelle, C. V.; Lecommandoux, S.; Gillies, E. R. Synthesis, Self-Assembly, and Degradation of Amphiphilic Triblock Copolymers with Fully Photodegradable Hydrophobic Blocks. *Can. J. Chem.* **2015**, *93*, 126−133.

(38) McBride, M. K.; Gong, T.; Nair, D. P.; Bowman, C. N. Photo-Mediated Copper(I)-Catalyzed Azide-Alkyne Cycloaddition (CuAAC) "Click" Reactions for Forming Polymer Networks as Shape Memory Materials. *Polymer* **2014**, *55*, 5880−5884.

(39) Tang, R.; Chen, H.; Zhou, S.; Xiang, W.; Tang, X.; Liu, B.; Dong, Y.; Zeng, H.; Li, Z. Dendronized Hyperbranched Polymers Containing Isolation Chromophores: Design, Synthesis and Further Enhancement of the Comprehensive Nlo Performance. *Polym. Chem.* **2015**, *6*, 5580−5589.

(40) Tang, R.; Chen, H.; Zhou, S.; Liu, B.; Gao, D.; Zeng, H.; Li, Z. The Integration of an "X" Type Dendron into Polymers to Further Improve the Comprehensive Nlo Performance. *Polym. Chem.* **2015**, *6*, 6680−6688.

DOI: 10.1021/acs.macromol.8b02671
Macromolecules 2019, 52, 1985−1992

(41) Wang, J.; Mei, J.; Zhao, E.; Song, Z.; Qin, A.; Sun, J.; Tang, B. Z. Ethynyl-Capped Hyperbranched Conjugated Polytriazole: Click Polymerization, Clickable Modification, and Aggregation-Enhanced Emission. *Macromolecules* **2012**, *45*, 7692−7703.
(42) Albayrak, C.; Swartz, J. R. Direct Polymerization of Proteins. *ACS Synth. Biol.* **2014**, *3*, 353−362.
(43) Shi, Y.; Cao, X.; Hu, D.; Gao, H. Highly Branched Polymers with Layered Structures That Mimic Light-Harvesting Processes. *Angew. Chem., Int. Ed.* **2018**, *57*, 516−520.
(44) Zou, L.; Shi, Y.; Cao, X.; Gan, W.; Wang, X.; Graff, R. W.; Hu, D.; Gao, H. Synthesis of Acid-Degradable Hyperbranched Polymers by Chain-Growth Cuaac Polymerization of an AB_3 Monomer. *Polym. Chem.* **2016**, *7*, 5512−5517.
(45) Han, J.; Zhu, D. D.; Gao, C. Fast Bulk Click Polymerization Approach to Linear and Hyperbranched Alternating Multiblock Copolymers. *Polym. Chem.* **2013**, *4*, 542−549.
(46) Wang, X.; Hu, R.; Zhao, Z.; Qin, A.; Tang, B. Z. Self-Healing Hyperbranched Polytriazoles Prepared by Metal-Free Click Polymerization of Propiolate and Azide Monomers. *Sci. China: Chem.* **2016**, *59*, 1554−1560.
(47) Qin, A.; Lam, J. W. Y.; Jim, C. K. W.; Zhang, L.; Yan, J.; Haussler, M.; Liu, J.; Dong, Y.; Liang, D.; Chen, E.; Jia, G.; Tang, B. Z. Hyperbranched Polytriazoles: Click Polymerization, Regioisomeric Structure, Light Emission, and Fluorescent Patterning. *Macromolecules* **2008**, *41*, 3808−3822.
(48) Brady, S. E.; Shultz, G. V.; Tyler, D. R. Preparation of Polymers Containing Metal-Metal Bonds Along the Backbone Using Click Chemistry. *J. Inorg. Organomet. Polym. Mater.* **2010**, *20*, 511−518.
(49) Wang, C.; Ikhlef, D.; Kahlal, S.; Saillard, J. Y.; Astruc, D. Metal-Catalyzed Azide-Alkyne "Click" Reactions: Mechanistic Overview and Recent Trends. *Coord. Chem. Rev.* **2016**, *316*, 1−20.
(50) Zhang, L.; Chen, X.; Xue, P.; Sun, H. H. Y.; Williams, I. D.; Sharpless, K. B.; Fokin, V. V.; Jia, G. Ruthenium-Catalyzed Cycloaddition of Alkynes and Organic Azides. *J. Am. Chem. Soc.* **2005**, *127*, 15998−15999.
(51) Boren, B. C.; Narayan, S.; Rasmussen, L. K.; Zhang, L.; Zhao, H.; Lin, Z.; Jia, G.; Fokin, V. V. Ruthenium-Catalyzed Azide-Alkyne Cycloaddition: Scope and Mechanism. *J. Am. Chem. Soc.* **2008**, *130*, 8923−8930.
(52) Liu, P.; Siyang, H.; Zhang, L.; Tse, S. K.; Jia, G. $RuH_2(CO)(PPh_3)_3$ Catalyzed Selective Formation of 1,4-Disubstituted Triazoles from Cycloaddition of Alkynes and Organic Azides. *J. Org. Chem.* **2012**, *77*, 5844−5849.
(53) Liu, P.; Li, J.; Su, F.; Ju, K.; Zhang, L.; Shi, C.; Sung, H. H. Y.; Williams, I. D.; Fokin, V. V.; Lin, Z.; Jia, G. Selective Formation of 1,4-Disubstituted Triazoles from Ruthenium-Catalyzed Cycloaddition of Terminal Alkynes and Organic Azides: Scope and Reaction Mechanism. *Organometallics* **2012**, *31*, 4904−4915.
(54) Hu, R.; Leung, N. L. C.; Tang, B. Z. AIE Macromolecules: Syntheses, Structures and Functionalities. *Chem. Soc. Rev.* **2014**, *43*, 4494−4562.
(55) Qin, A.; Lam, J. W. Y.; Tang, B. Z. Luminogenic Polymers with Aggregation-Induced Emission Characteristics. *Prog. Polym. Sci.* **2012**, *37*, 182−209.
(56) Mei, J.; Leung, N. L. C.; Kwok, R. T. K.; Lam, J. W. Y.; Tang, B. Z. Aggregation-Induced Emission: Together We Shine, United We Soar! *Chem. Rev.* **2015**, *115*, 11718−11940.
(57) Liu, B.; Pucci, A.; Baumgartner, T. Aggregation Induced Emission: A Land of Opportunities. *Mater. Chem. Front.* **2017**, *1*, 1689−1690.
(58) Liang, J.; Tang, B. Z.; Liu, B. Specific Light-up Bioprobes Based on AIEgen Conjugates. *Chem. Soc. Rev.* **2015**, *44*, 2798−2811.
(59) Bryce, M. R. Aggregation-Induced Delayed Fluorescence (AIDF) Materials: A New Break-through for Nondoped Oleds. *Sci. China: Chem.* **2017**, *60*, 1561−1562.
(60) Wu, Y.; Qin, A.; Tang, B. Z. AIE-Active Polymers for Explosive Detection. *Chin. J. Polym. Sci.* **2017**, *35*, 141−154.
(61) Han, T.; Jim, C. K. W.; Lam, J. W. Y.; Tang, B. Z. Polyynes with Aggregation-Induced Emission Characteristics: Synthesis and Their Photonic Properties. *Acta Chim. Sin.* **2016**, *74*, 877−884.
(62) Qin, A.; Lam, J. W. Y.; Tang, L.; Jim, C. K. W.; Zhao, H.; Sun, J.; Tang, B. Z. Polytriazoles with Aggregation-Induced Emission Characteristics: Synthesis by Click Polymerization and Application as Explosive Chemosensors. *Macromolecules* **2009**, *42*, 1421−1424.
(63) Wang, J.; Mei, J.; Yuan, W.; Lu, P.; Qin, A.; Sun, J.; Ma, Y.; Tang, B. Z. Hyperbranched Polytriazoles with High Molecular Compressibility: Aggregation-Induced Emission and Superamplified Explosive Detection. *J. Mater. Chem.* **2011**, *21*, 4056−4059.
(64) Qin, A.; Tang, L.; Lam, J. W. Y.; Jim, C. K. W.; Yu, Y.; Zhao, H.; Sun, J.; Tang, B. Z. Metal-Free Click Polymerization: Synthesis and Photonic Properties of Poly(aroyltriazole)s. *Adv. Funct. Mater.* **2009**, *19*, 1891−1900.
(65) Li, H.; Wang, J.; Sun, J.; Hu, R.; Qin, A.; Tang, B. Z. Metal-Free Click Polymerization of Propiolates and Azides: Facile Synthesis of Functional Poly(aroxycarbonyltriazole)s. *Polym. Chem.* **2012**, *3*, 1075−1083.
(66) Wu, Y.; He, B.; Quan, C.; Zheng, C.; Deng, H.; Hu, R.; Zhao, Z.; Huang, F.; Qin, A.; Tang, B. Z. Metal-Free Poly-Cycloaddition of Activated Azide and Alkynes toward Multifunctional Polytriazoles: Aggregation-Induced Emission, Explosive Detection, Fluorescent Patterning, and Light Refraction. *Macromol. Rapid Commun.* **2017**, *38*, 1700070.
(67) Zhao, E.; Li, H.; Ling, J.; Wu, H.; Wang, J.; Zhang, S.; Lam, J. W. Y.; Sun, J.; Qin, A.; Tang, B. Z. Structure-Dependent Emission of Polytriazoles. *Polym. Chem.* **2014**, *5*, 2301−2308.
(68) Zhang, G.; Chen, Z.; Aldred, M. P.; Hu, Z.; Chen, T.; Huang, Z.; Meng, X.; Zhu, M. Q. Direct Validation of the Restriction of Intramolecular Rotation Hypothesis Via the Synthesis of Novel Ortho-Methyl Substituted Tetraphenylethenes and Their Application in Cell Imaging. *Chem. Commun.* **2014**, *50*, 12058−12060.
(69) Zhao, Z.; He, B.; Nie, H.; Chen, B.; Lu, P.; Qin, A.; Tang, B. Z. Stereoselective Synthesis of Folded Luminogens with Arene-Arene Stacking Interactions and Aggregation-Enhanced Emission. *Chem. Commun.* **2014**, *50*, 1131−1133.
(70) Higashihara, T.; Ueda, M. Recent Progress in High Refractive Index Polymers. *Macromolecules* **2015**, *48*, 1915−1929.
(71) Liu, J.; Ueda, M. High Refractive Index Polymers: Fundamental Research and Practical Applications. *J. Mater. Chem.* **2009**, *19*, 8907−8919.
(72) Refractive index database: http://refractiveindex.info (accessed: September, 2018).

DOI: 10.1021/acs.macromol.8b02671
Macromolecules 2019, 52, 1985−1992